

Specific Heat of Nanofluids—An Experimental Investigation



Tushar Anand and Soumya Suddha Mallick

1 Introduction

Nanofluids are a new class of engineered fluids obtained by suspending nano-size (10^{-9} m) particles with an average size below 100 nm in heat transfer fluids [1]. Oxides, metals, nitrides, and non-metals, such as carbon nanotubes are used as nanoparticles, while water, ethylene glycol, oils, and polymer solutions, and conventional coolants are used as base fluids. The smaller size of nanofluids offers several advantages over conventional heat transfer fluids, such as long-term stability, low abrasion, low pumping power, homogeneity, and minimum clogging in flow passages [2, 3]. These benefits make nanofluids potentially attractive to various industries having heat transfer applications like microelectronics, transportation, biomedical, micro-fluids, nuclear, automobile, power generation, X-ray, refrigerators, etc. [4, 5]. Miniaturized systems will reduce heat transfer fluid inventory and successful employment of nanofluids will result in significant energy and cost savings because heat exchange systems can be made smaller and lighter [6].

Despite such merits and widespread potential applications of nanofluids, nanofluid technology is still limited for commercial use because there is yet no proven standardized design process for accurately predicting important heat transfer properties, such as the nanofluids specific heat, thermal conductivity, and viscosity because of the influence of various particle and fluid properties, such as the shape and size distribution of nanoparticles [7, 8], the volume concentration of nanoparticles in base fluids [9, 10], ultrasonication and storage time to prepare nanofluids [9], use of surfactants [7, 10], pH value [3] and temperature [7, 10]. Developing an accurate fundamental model for the specific heat of nanofluids is a challenging task. As a thermodynamic

T. Anand (✉)

Satyug Darshan Institute of Engineering and Technology, Faridabad 121002, India

S. S. Mallick

Mechanical Engineering Department, Thapar University, Patiala 147001, India

e-mail: ssmallick@thapar.edu

property, the specific heat capacity of a nanofluid dictates the nanoparticle and fluid temperature changes, which affect the temperature field of the nanofluid, and hence, the heat transfer and flow status in any application, e.g., systems for utilizing low-temperature solar thermal energy, include means for heat collection, usually heat storage, either short-term or interseasonal and distribution within a structure or a district heating network [11].

Hence, the purpose of this paper is to first construct a setup and validate it. Secondly, to carry out experimental work to find out the effect of different particle sizes, volumetric concentration, sonication time, frequency of the specific heat of different nanofluid. Thirdly, to develop an improved model for specific heat using the data obtained.

2 Experimental Setup and Procedure

The experimental setup used is shown in Fig. 1. The apparatus consists of a 20 cm long and 7 cm inside borosilicate container. The apparatus is designed to hold about 900 ml of liquid. The nanofluids are heated from about 298–323 K by using an electrical immersion heater. Ten *K* type copper–constantan thermocouples place in the apparatus. Four thermocouples are placed within the liquid volume to get the average temperature of the liquid. One on the heating coil, two thermocouples are placed on the outer surface of the container, two on the outer surface of second insulation, and one at the midpoint of the last insulation coil. These thermocouples are connected to a data logger that records the temperature data at every 15 s interval.

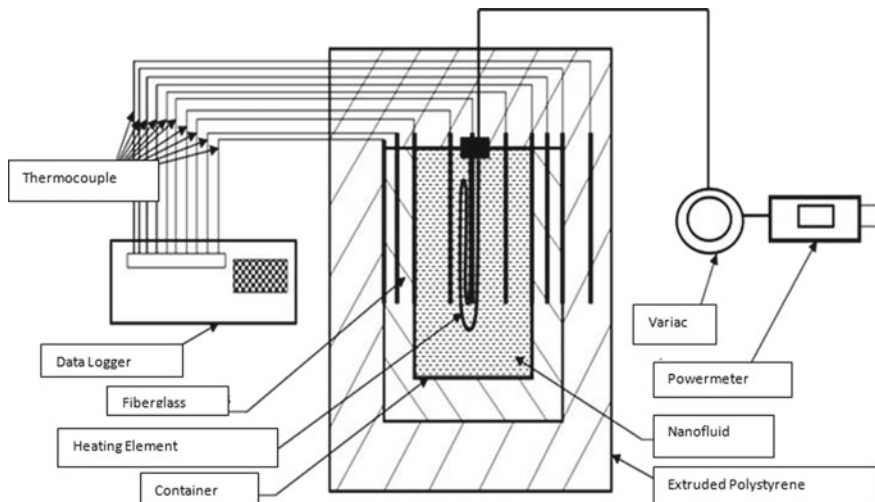


Fig. 1 Layout of experimental setup for specific heat

The container is well insulated to minimize heat loss. The specific heat of a nanofluid was calculated from the following equation:

$$C_{\text{Pnf}} = \frac{Q\Delta t - m_C C_{\text{PC}} \Delta T_C - m_{\text{co}} C_{\text{PCO}} \Delta T_{\text{CO}} - m_{\text{in}} C_{\text{PIN}} - q_L \Delta t}{m_{\text{nf}} \Delta T_{\text{nf}}} \quad (1)$$

where Q is the heat applied to the electrical heater in watts determined from the power meter. The time interval t is measured by the data logger s , T is the temperature rise K , m is the mass in kg , C_p is the specific heat kJ/kgK , and q_L is the heat transfer to the environment (W). The subscripts C represents the container, CO the heating coil, and IN the insulation. The masses of the container, coil, and insulation are measured individually by an electronic mass balance. The temperature range ΔT is recorded every 15 s intervals. The data values used are taken from standard sources. The setup has been validated satisfactorily with experiments on water and ethyl glycol (25, 30, and 50%).

3 Modeling

There are two specific heat models widely used in the nanofluid literature. The model I is similar to mixing theory for ideal gas mixtures [12]. This is macroscopic, that is, the specific heat capacity of a nanofluid is equal to the average of the specific heat capacities of base fluid and nanoparticles.

$$C_{\text{Pnf}} = \phi C_{\text{Ps}} + (1 - \phi) C_{\text{Pbf}} \quad (2)$$

Model II [7] is based on the assumption of thermal equilibrium between the particles and the surrounding fluid. This is microscopic, which assumes the base fluid and the nanoparticles are in their thermal equilibrium. The nanofluid specific heat capacity per unit mass of nanofluid, that is, the nanofluid specific heat, is

$$C_{\text{Pnf}} = \frac{C_{\text{ps}} \phi \rho_s + (1 - \phi) \rho_{\text{bf}} C_{\text{Pbf}}}{\rho_{\text{nf}}} \quad (3)$$

where ρ_s is the density of the solid nanoparticle, ρ_{bf} is the density of the base fluid, and ρ_{nf} is the density of the nanofluid. The product of density and specific heat is the volumetric heat capacity of each constituent and that of the nanofluid.

3.1 Evaluation of Existing Models

Models given in Eqs. (2) and (3) are being compared with the experimental data for the same range of volume fraction, temperature, and particle size. Lines of best fit

have been drawn through the experimental data to indicate their trends. The following parameters are considered for calculation in this paper (Figs. 2 and 3):

Specific heat and density of water areas 4.186 kJ/kgK and 1000 kg/m³, respectively; (b) density of Al₂O₃ particles were as mentioned in their respective references, such as ρ_p : 3965 kg/m³; (c) specific heat of Al₂O₃ is 880 J/kg K;

With an increase in the nanoparticle volume fraction, the predicted values increase for all the models; also, the number of inaccuracy increases. It is seen that the above models do not fit the experimental data; therefore, a model using the dimensional analysis was used to develop a correlation fitting the experimental data. The variables like diameter, temperature, the viscosity of the fluid, the density of the particle, base

Fig. 2 Al₂O₃ nanoparticles, d : 50 nm, T : 35 °C

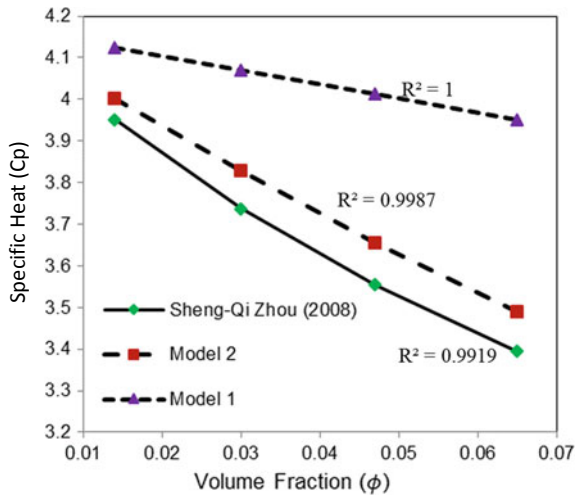
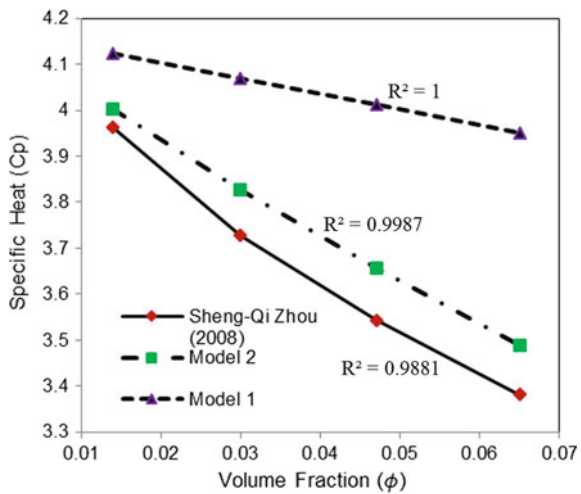


Fig. 3 Al₂O₃ nanoparticles, d : 50 nm, T : 55 °C



fluid, volume fraction, the specific heat of nanoparticle and that of nanofluid are taken. Specific heat of nanofluid is believed to be depending on various particle and fluid properties, as given by:

$$C_{Pnf} = f(d, T, \mu, \rho_f, \rho_p, C_{PP}, C_{Pf}, \phi) \tag{4}$$

Or

$$f_1(d, T, \mu, \rho_f, \rho_p, C_{PP}, C_{Pf}, \phi)$$

Using Buckingham P_i theorem, the following dimensionless groups have been obtained:

$$\pi_1 = \frac{d^2 T \rho_p^2 C_{Pf}}{\mu^2}, \pi_2 = \frac{\rho_f}{\rho_p}, \pi_3 = \frac{d^2 T \rho_p^2 C_{Pp}}{\mu^2},$$

$$\pi_4 = \frac{d^2 T \rho_p^2 C_{Pf}}{\mu^2}, \pi_5 = \phi$$

Experimental data for Al_2O_3 -water nanofluids ZnO-water nanofluids and SWCNT for a wide range of volume fraction, particle size, and temperature, the following models have been derived using regression analysis. Finally, the specific heat of nanofluid from the dimensionless analysis is as shown in (Fig. 4).

$$C_{nf} = 0.152 \frac{\mu^2}{d^2 T \rho_p^2} \left(\frac{\rho_f}{\rho_p} \right)^{2.28} \left(\frac{d^2 T \rho_p^2 C_{Pp}}{\mu^2} \right)^{-1.62} \left(\frac{d^2 T \rho_p^2 C_{Pf}}{\mu^2} \right)^{2.81} \phi \tag{5}$$

The model given in Eq. (5) is for Al_2O_3 -water nanofluids, ZnO, and SWCNT. The temperature range for which the relation is valid up to 338 K.

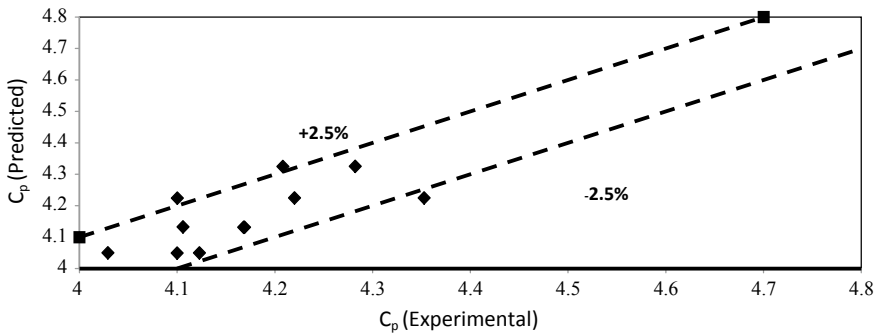


Fig. 4 Experimental versus predicted values of specific heat for Al_2O_3 -water (alpha) nanofluids using a new model given (Eq. 5)

The above models have been used to predict the nanofluid specific heat between predicted and experimental values for Al_2O_3 -water (alpha) nanofluids. The comparison plots show that the new model generally predicts within $\pm 2.5\%$ accuracy range for Al_2O_3 -water (alpha) nanofluids

Figure 5: Comparison between experimental and predicted plots shows that the new model generally predicts within $\pm 5\%$ accuracy range for Al_2O_3 -water (gamma) nanofluids

Figure 6: Comparison between experimental and predicted plots shows that the new model generally predicts within $\pm 5\%$ accuracy range for ZnO (14 nm) nanofluids

Figure 7: Comparison between experimental and predicted plots shows that the new model generally predicts within $\pm 3\%$ accuracy range for ZnO (14 nm) nanofluids

Fig. 5
 Al_2O_3 -water(gamma)
nanofluids using a new
model given Eq. (5)

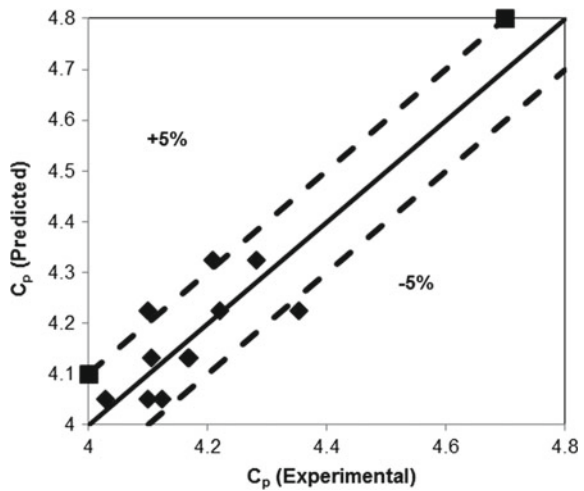


Fig. 6 ZnO (14 nm)
nanofluids using a new
model given Eq. (5)

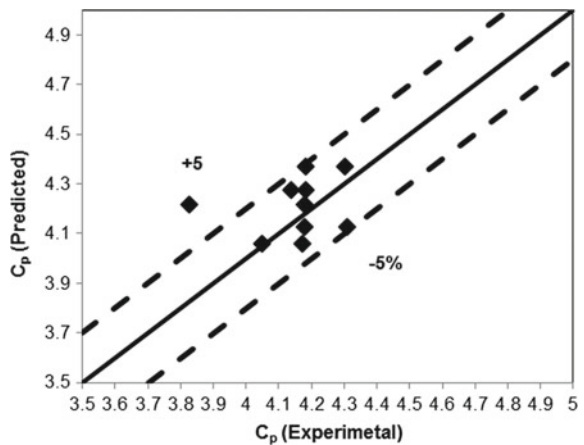


Fig. 7 ZnO (24 nm) nanofluids using a new model given (Eq. 5)

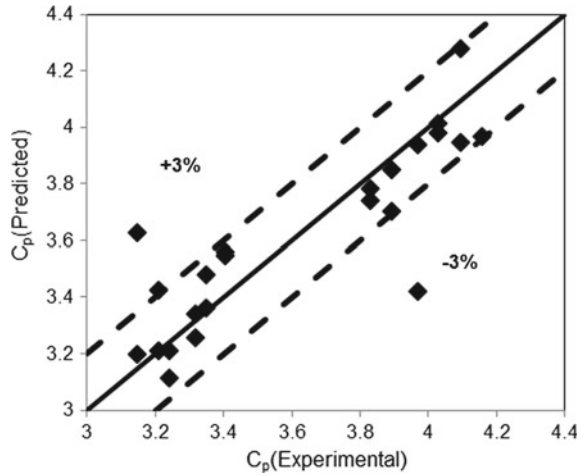


Fig. 8 SWCNT (1 nm) nanofluids using a new model given (Eq. 5)

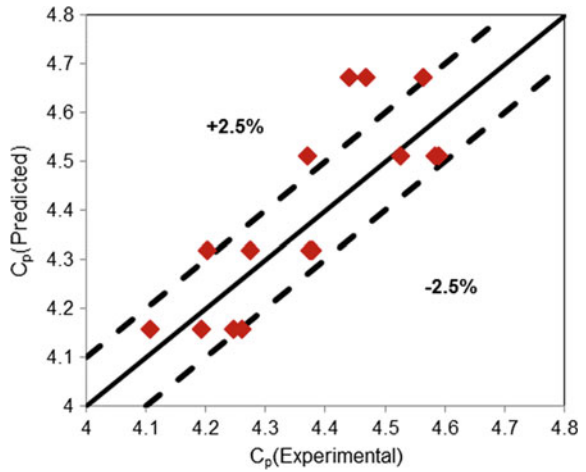


Figure 8: Comparison between experimental and predicted plots shows that the new model generally predicts within $\pm 2.5\%$ accuracy range for SWCNT (1 nm) nanofluids

4 Uncertainty Analysis

The uncertainty in the specific heat of the experimental data measurement in Eq. (1) can be determined from the standard approach presented by [13]. The parameters

measured are the rate of heat input to the nanofluid, the temperature, and the mass of several objects and dimensions of insulations.

$$\frac{\delta C_{\text{pnf}}}{C_{\text{pnf}}} = \left[\left(\frac{\delta Q}{Q} \right)^2 + \left(\frac{\delta m_c}{m_c} \right)^2 + \left(\frac{\delta \Delta T_C}{m_C} \right)^2 + \left(\frac{\delta m_{\text{CO}}}{m_{\text{CO}}} \right)^2 + \left(\frac{\delta \Delta T_{\text{CO}}}{\Delta T_{\text{CO}}} \right)^2 + \left(\frac{\delta m_{\text{IN}}}{m_{\text{IN}}} \right)^2 + \left(\frac{\delta \Delta T_{\text{IN}}}{\Delta T_{\text{IN}}} \right)^2 + \left(\frac{\delta q_L}{Q} \right)^2 + \left(\frac{\delta m_{\text{nf}}}{m_{\text{nf}}} \right)^2 + \left(\frac{\delta \Delta T_{\text{nf}}}{\Delta T_{\text{nf}}} \right)^2 \right]^{1/2} \quad (6)$$

Specific heats of the container, heating element, and insulations were directly read from tabulated values in books and were not measured quantities in this experiment. The data acquisition system was capable of sampling temperatures at intervals of microseconds. Therefore, the uncertainty in Δt of 15 s was considered negligible. For the power meter, $\delta Q/Q$ is about 1%. For the electronic precision, mass balance is $\delta m/m$ about 0.5%. The uncertainty in measurements of temperature for copper–constantan thermocouple used in this apparatus is 0.5 °C between -100 and 400 °C. Therefore, at the mean temperature of 50 °C within the range of measurements, $\delta t/t = 1\%$. The uncertainty in calculating the heat loss through the insulation can be expressed as Eq. (7)

$$\left(\frac{\delta q_L}{q_L} \right) = \left[\left(\frac{\delta A}{A} \right)^2 + \left(\frac{\delta T_C}{T_C} \right)^2 + \left(\frac{\delta T_O}{T_O} \right)^2 + \left(\frac{\delta X_1}{X_1} \right)^2 + \left(\frac{\delta X_2}{X_2} \right)^2 \right]^{1/2} \quad (7)$$

where X_1 and X_2 are thicknesses of insulations, and T_C and T_O are the surface temperatures of insulations. The thermal conductivities of insulations are taken from Incropera, [14]. The uncertainty in length measurement $\delta L/L$ by the modern meteorological gauge is about 0.5%. The area A is proportional to the square of the length dimension L , so the uncertainty in area measurement is $[(2(\delta L/L))]^{1/2}$. Using the above numbers, $\delta q_L/q_L = 1.87\%$. Finally, combining all the uncertainties together in Eq. (6), the uncertainty in measurement of the specific heat of nanofluid is $\delta C_{\text{pnf}}/C_{\text{pnf}} = 3.1\%$.

5 Conclusions

1. The specific heat of nanofluids increases with an increase in temperature and volume fraction. For example, Al_2O_3 (0.0014%) at 302 K is 4.4 kJ/kgK, and at 303 K, it is 5.1 kJ/kgK, ZnO; at 0.001%, volume fraction is 3.7 kJ/kgK, and at 0.002% is 4.03 kJ/kgK.
2. A new specific heat model has been developed using dimensionless analysis. The new model has been found to generally predict specific heat of nanofluids within

±2.5% accuracy range for Al₂O₃-water nanofluids,
 ± 5% accuracy range for ZnO-water nanofluids and
 ± 5% accuracy range for SWCNT.

3. The newly developed model gave good results when compared with models of different nanofluid of SWCNT, Al₂O₃, ZnO, ethyl glycol up to the temperature range of 298–308 K.

Acknowledgements The authors are very thankful to Dr. N J Dembi for his important suggestion regarding this paper and Thapar University for its seed money.

References

1. Choi SUS (1999) Nanofluid Technology: current status and future research. Energy technology division, Argonne national laboratory, IL, p 60439
2. Gallego MJP, Lugo L, Legido JL, Pineiro MM (2008) Thermal conductivity and viscosity measurements of ethylene glycol-based Al₂O₃ nanofluids. *Nanoscale Res Lett* 6(211):1–11
3. Xie HQ, Wang JC, Xi TG, Liu Y, Ai F, Wu QR (2002) Thermal conductivity enhancement of suspensions containing nanosized alumina particles. *Appl Phys* 91(7):4568–4572
4. Chandrasekar M, Suresh S, Bose AC (2010) Experimental investigations and theoretical determination of thermal conductivity and viscosity of Al₂O₃ water
5. Khanafer K, Vafai K (2011) A critical synthesis of thermophysical characteristics of nanofluids. *Int J Heat Mass Trans* 54:4410–4428
6. Parashivamurthy KI (2010) International conference on advanced materials, manufacturing, management and thermal science, Department of Mechanical Engineering, Siddaganga Institute of Technology, Tumkur-572104, Karnataka, India, vol 1
7. Murshed SMS, Leong KC, Yang C (2005) Enhanced thermal conductivity of TiO₂-water-based nanofluids. *Int J Therm Sci* 44:367–373
8. Wang ZL, Tang DW, Liu S, Zheng XH, Araki N (2007) Thermal-conductivity and thermal-diffusivity measurements of nanofluids by 3 ω method and mechanism analysis of heat transport. *Thermophys* 28:1255–1268
9. Timofeeva EV, Gavrillov AN, McCloskey JM, Tolmachev YV, Sprunt S, Lopatina LM, Selinger JV (2007) Thermal conductivity and particle agglomeration in alumina nanofluids: experiment and theory. *Phys Rev E* 76(061703):1–16
10. Madhu P, Rajasekhar PG (2017) Measurement of density and specific heat capacity of different nanofluids. *IJARIIIT*. ISSN: 2454-132X. 165–170
11. Vajjha RS, Das DK (2009) Specific heat measurement of three nanofluids and development of new correlations. *J Heat Transfer* 131(7):071601
12. Das SK, Choi SUS, Yu W, Pradeep K (2007) *Nanofluids science and technology*, Wiley interscience. *Appl Phys* 9:131–139
13. Coleman HW, Steele WG (1999) *Experimentation and uncertainty analysis for engineers*, 2nd edn. Wiley, New York
14. Incropera FP, DeWitt DP (1996) *Introduction to heat transfer*, 3rd edn. Wiley, New York
15. Chon CH, Kihm KD, Lee SP, Choi SUS (2005) Empirical correlation finding the role of temperature and particle size for nanofluid (Al₂O₃) thermal conductivity enhancement. *Phys Lett* 87(153107):1–3

16. Mints HA, Roy G, Nguyen CT (2007) New temperature-dependent thermal conductivity data of water-based nanofluids. In: 5th IASME/WSEAS international conference on heat transfer, thermal engineering and environment, Athens, Greece, pp 290–294
17. Das SK, Putra N, Thiesen P, Roetzel W (2003) Temperature dependence of thermal conductivity enhancement for nanofluids, heat transfer. *J Heat Transf* 125:567–574